5-2018

Measuring the Double Layer Capacitance of Electrolytes with Varied Concentrations

Geoffrey Rath
Linfield College

Recommended Citation

Rath, Geoffrey, "Measuring the Double Layer Capacitance of Electrolytes with Varied Concentrations" (2018). *Senior Theses*. 34.
https://digitalcommons.linfield.edu/physstud_theses/34

Measuring the Double Layer Capacitance of Electrolytes with Varied Concentrations

Geoffrey T. Rath

A THESIS
Submitted to
The Department of Physics
LINFIELD COLLEGE
McMinnville, Oregon

In partial fulfillment
of the requirements for the degree of

BACHELOR OF SCIENCE

May, 2018

THESIS COPYRIGHT PERMISSIONS

Please read this document carefully before signing. If you have questions about any of these permissions, please contact the DigitalCommons Coordinator.

Title of the Thesis:
Measuring the Double Layer Capacitance of Electrolytes with Varied Concentrations

Author's Name: (Last name, first name)
Rath, Geoffrey

Advisor's Name
Dr. Michael S. Crosser

DigitalCommons@Linfield (DC@L) is our web-based, open access-compliant institutional repository for digital content produced by Linfield faculty, students, staff, and their collaborators. It is a permanent archive. By placing your thesis in DC@L, it will be discoverable via Google Scholar and other search engines. Materials that are located in DC@L are freely accessible to the world; however, your copyright protects against unauthorized use of the content. Although you have certain rights and privileges with your copyright, there are also responsibilities. Please review the following statements and identify that you have read them by signing below. Some departments may choose to protect the work of their students because of continuing research. In these cases, the project is still posted in the repository but content will only be accessible by individuals who are part of the Linfield community.

CHOOSE THE STATEMENT BELOW THAT DEFINES HOW YOU WANT TO SHARE YOUR THESIS. THE FIRST STATEMENT PROVIDES THE MOST ACCESS TO YOUR WORK; THE LAST STATEMENT PROVIDES THE LEAST ACCESS. CHOOSE ONLY ONE STATEMENT.

X I **agree** to make my thesis available to the Linfield College community and to the larger scholarly community upon its deposit in our permanent digital archive, DigitalCommons@Linfield, or its successor technology. My thesis will also be available in print at Nicholson Library and can be shared via interlibrary loan.

OR

_____ I **agree** to make my thesis available **only** to the Linfield College community upon its deposit in our permanent digital archive, DigitalCommons@Linfield, or its successor technology. My thesis will also be available in print at Nicholson Library and can be shared via interlibrary loan.

OR

_____ I **agree** to make my thesis available in print at Nicholson Library, including access for interlibrary loan.

OR

_____ I **agree** to make my thesis available in print at Nicholson Library only.

Updated April 25, 2018

NOTICE OF ORIGINAL WORK AND USE OF COPYRIGHT-PROTECTED MATERIALS:

If your work includes images that are not original works by you, you must include permissions from the original content provider or the images will not be included in the repository. If your work includes videos, music, data sets, or other accompanying material that is not original work by you, the same copyright stipulations apply. If your work includes interviews, you must include a statement that you have the permission from the interviewees to make their interviews public. For information about obtaining permissions and sample forms, see https://copyright.columbia.edu/basics/permissions-and-licensing.html.

NOTICE OF APPROVAL TO USE HUMAN OR ANIMAL SUBJECTS:

If your research includes human subjects, you must include a letter of approval from the Linfield Institutional Review Board (IRB); see https://www.linfield.edu/faculty/irb.html for more information. If your research includes animal subjects, you must include a letter of approval from the Linfield Animal Care & Use Committee.

NOTICE OF SUBMITTED WORK AS POTENTIALLY CONSTITUTING AN EDUCATIONAL RECORD UNDER FERPA:

Under FERPA (20 U.S.C. § 1232g), this work may constitute an educational record. By signing below, you acknowledge this fact and expressly consent to the use of this work according to the terms of this agreement.

BY SIGNING THIS FORM, I ACKNOWLEDGE THAT ALL WORK CONTAINED IN THIS PAPER IS ORIGINAL WORK BY ME OR INCLUDES APPROPRIATE CITATIONS AND/OR PERMISSIONS WHEN CITING OR INCLUDING EXCERPTS OF WORK(S) BY OTHERS.

IF APPLICABLE, I HAVE INCLUDED AN APPROVAL LETTER FROM THE IRB TO USE HUMAN SUBJECTS OR FROM ANIMAL CARE & USE TO USE ANIMAL SUBJECTS.

Signature *Signature redacted* Date 5/22/18

Printed Name Geoffrey Rath

Approved by Faculty Advisor *Signature redacted* Date 5/22/18

Updated April 25, 2018

Thesis Acceptance

Linfield College

Thesis Title: Measuring the Double Layer Capacitance of Electrolytes with Varied Concentrations

Submitted by: Geoffrey T. Rath

Date Submitted: May, 2018

Thesis Advisor: Signature redacted

Dr. Michael S. Crosser

Physics Department: Signature redacted

Dr. Jennifer Heath

Physics Department: Signature redacted

Dr. Joelle Murray

Abstract

When electric potentials are applied from an electrolytic fluid to a metal, a double layer capacitor, C_{dl}, develops at the interface. The layer directly at the interface is called the Stern layer, and has a thickness equal to roughly the size of the ions in the fluid. The next layer, the diffuse layer, arises from the gathering of like charges in the Stern layer. This layer is the distance needed for ionic charges to return to equilibrium. This distance, called the Debye length, λ, depends on the square root of the electrolyte concentration. To study the properties of the diffuse layer, we measure C of a cylindrical capacitor using different concentrations of electrolyte solutions in the system we machined. We found that the initial model, which only depended on the Debye length, was not sufficient to predict the capacitance in complex electrolytes where the Stern layer was not nearly symmetric.

Table of Contents

1. Background 1

  1.1 Supercapacitors...1

  1.2 Properties of Ionic Fluids..1

  1.3 Double Layer Capacitance...2

2. Experiment 3

  2.1 Electrolytic Solutions...3

    2.1.1 Conductivity Probe 4

  2.2 Brass Macro Capacitor..5

3. Theory 8

  3.1 Cylindrical Capacitance 8

  3.2 Double Layer Capacitors 8

    3.2.1 Debye Length..9

    3.2.2 Stern Layer...9

  3.3 Total Capacitance...9

  3.4 Stern Layer Inclusion..10

4. Results & Analysis 13

  4.1 NaCl 13

    4.1.1 Linear Capacitance..13

    4.1.2 $\sqrt{c}$ Dependency 14

  4.2 Phosphate 15

    4.2.1 Linear Capacitance..15

4.2.2 $\sqrt{c}$ Dependency 16

4.3 HEPES 16

4.3.1 Linear Capacitance 17

4.3.2 $\sqrt{c}$ Dependency 17

4.4 Discussion 18

5. Conclusions 19

6. Acknowledgements 20

7. Bibliography 21

List of Figures

Figures

1.1 Graphic of Double Layer Capacitance 2

2.1 Fluid Distribution and Micropipette 3

2.2 Linearity of Conductivity vs Concentration 4

2.3 Macro Device Image and Schematic 5

2.4 Sample Data 6

2.5 Experimental Setup 7

3.1 Model of Double Layer Capacitance with Stern & Debye 10

4.1 Linear Capacitance of NaCl 14

4.2 $\sqrt{c}$ Fit of NaCl 14

4.3 Linear Capacitance of Phosphate 15

4.4 $\sqrt{c}$ Fit of Phosphate 16

4.5 Linear Capacitance of HEPES 17

4.6 $\sqrt{c}$ Fit of HEPES 17

1. Background

This thesis will endeavor to analyze the intrinsic properties of electrolytic fluids on a macroscopic scale. To accomplish this, a cylindrical capacitor will be used. The design and mathematics behind this system can be found in the experiment section. Fluid capacitors are quickly becoming a prevalent way of storing energy, and a better understanding of different electrolytes could lead to better and more efficient devices.

1.1 Supercapacitors

The principles behind a supercapacitor are not too different from those of simple parallel plate capacitors. Instead of just a single set of plates, multiple capacitors are stacked on top of each other, separated by a small non-conducting separator. This allows the system to store up much larger quantities of energy in a much more compact system.

Supercapacitors have a wide variety of applications, from transportation to energy harvesting. Initially supercapacitors were only used for memory storage or smaller electronic purposes. With improvements to the technology, supercapacitors have found their way into hybrid cars, improving the battery life and capturing energy for short term usage. They have also been applied to solar arrays and are a candidate to replace the lithium battery.[6]

1.2 Properties of Ionic Fluids

Ionic fluids contain ions that function as the charge carrier for the fluid. The amount of carriers depends on the concentration of the fluid. In this experiment ionic salts are used so the concentration of salt in the water will determine the amount of ionic carriers[2]. When exposed to an external voltage the ionic fluid in a capacitor creates an effect called double layer capacitance.

1.3 Double Layer Capacitance

Double layer capacitance is only found in ionic fluid capacitors. The primary functionality behind the behavior is that the metal and fluid use different charge carriers, which are allowed to interact but cannot cross the boundary. The charged plates attract the oppositely charged ions and these ions gather at the interface. This separation of charge creates a capacitance and this is called the double layer capacitance. Double layer capacitance is discussed in more detail in section 3.2.

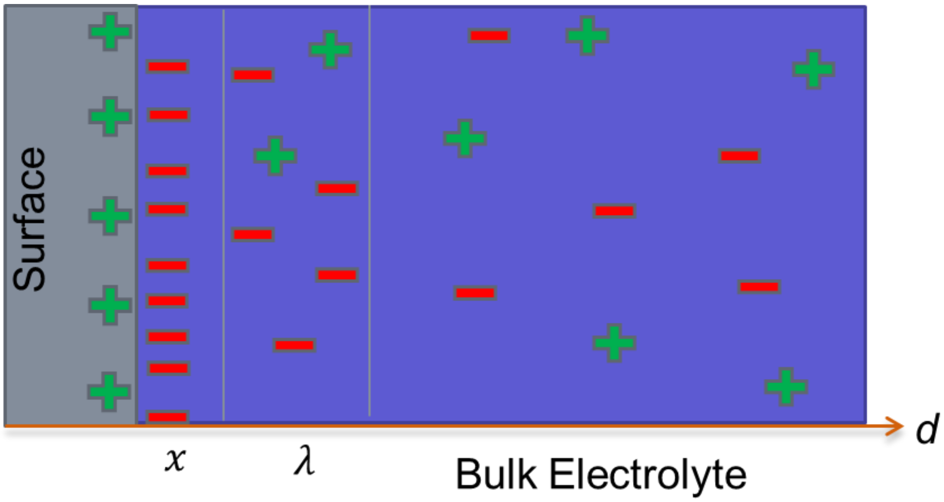

Figure 1.1: Graphic depicting the interaction of a double layer capacitor at the interface of a metal, where *x* is the width of the Stern layer and λ is the Debye length.

2. Experiment

2.1 Electrolytic Solutions

To determine the relationships between double layer capacitance and ionic concentration it is important to have varied ionic solutions at known concentrations. The solutions used in this experiment are all ionic salts. NaCl, a phosphate buffer KH_2PO_4, and HEPES buffer were all dried in an oven at 413K for three hours before being combined with deionized, DI, water. To obtain the desired initial concentration of 250mM for the HEPES and 500mM for NaCl and phosphate the required mass of salt is calculated from the molarity equations.

$$\textbf{Moles (mol)} = \frac{\textbf{Mass (g)}}{\textbf{Molar Mass}\left(\frac{\textbf{g}}{\textbf{mol}}\right)} \tag{1}$$

$$\textbf{Molarity (mM)} = \frac{\textbf{Moles of Solute (mol)}}{\textbf{Volume of Solution (mL)}} \tag{2}$$

The solutions are then diluted to the desired concentrations in mM using baked glassware. The desired concentrations for our experiment are: 5, 2.5, 1.25, 0.5, 0.25, 0.125, 0.05mM. This can be easily obtained by doing two half dilutions from 5 to 2.5 to 1.25 and then tenth dilutions for the remaining fluids.

Figure 2.1: NaCl fluid dilutions and micropipette.

2.1.1 Conductivity Probe

The use of a conductivity probe ensures that fluid concentrations are within their expected ranges. The probe was tested for consistency by checking its reading for deionized water in both a steady stream and small bursts. The probe was dipped into each fluid and measurements taken. After each test the probe was rinsed with DI water and dried using Nitrogen gas. Measurements were taken from lowest to highest concentration to minimalize chance of contamination. The conductivity probe was overloaded at the highest electrolyte concentrations but all others were consistent with expectations. Since the other dilutions are as expected, we assume that the higher order concentrations are also accurate.

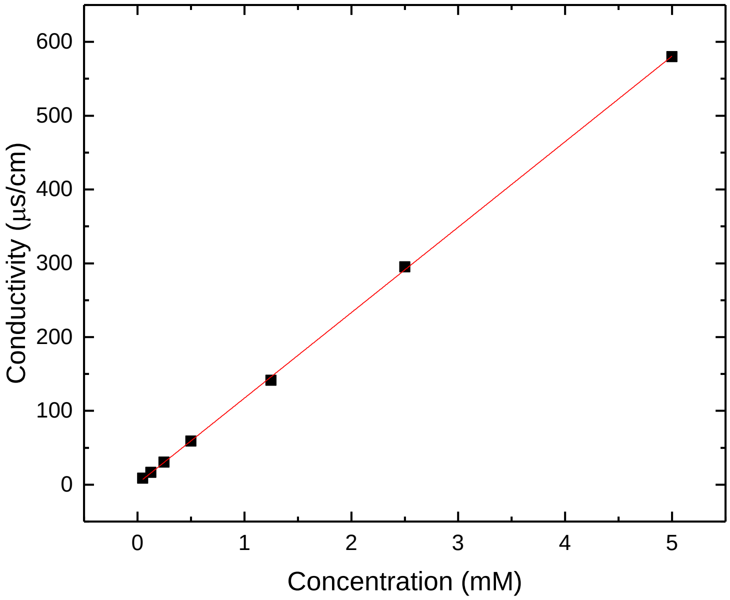

Figure 2.2: Data showing a strong linear correlation between measured conductivities and concentration (black squares), with a linear curve fit (linear line).

2.2 Brass Macro Capacitor

To analyze the fluids on the macroscopic scale a brass cylindrical capacitor was manufactured. The design consisted of three machined parts: A Garolite base, which was chosen for the base due to its insulating and chemically nonreactive properties. The inner cylinder, and outer ring which were machined from brass and was chosen because it is an easy conductor to machine. The pieces were assembled using three screws. One fits the central cylinder to the base and two outer screws seal the outer ring. In between the Garolite and brass is a thin piece of parafilm that acts as a seal to keep the system from leaking. A schematic and actual image can be seen in Figure 2.3.

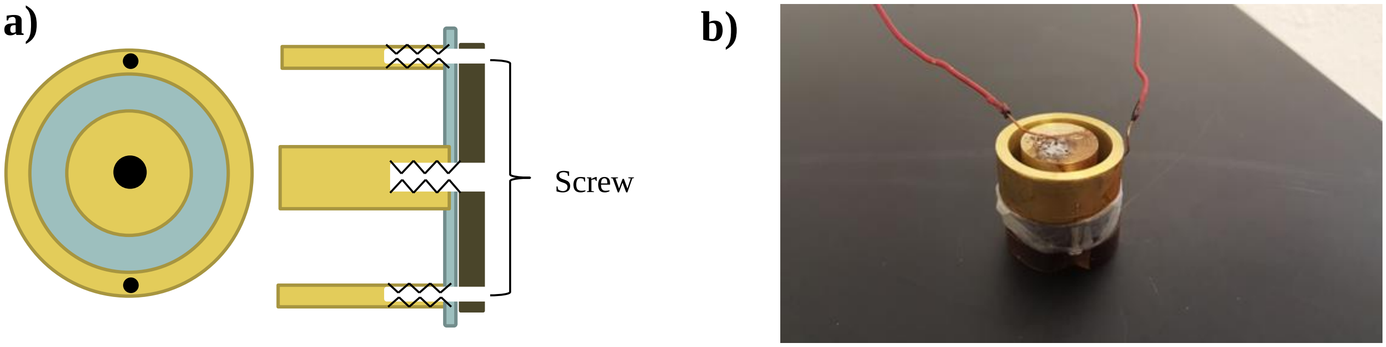

Figure 2.3: a) Schematic of the cylindrical capacitor design and b) actual image of completed capacitor.

The device was machined in a lathe using 1.25’’ brass cylindrical rod and Garolite rod. A narrow boring bar was implemented to hollow out the middle of the brass cylinder, leaving a center column of material. The inner and outer cylinders were parallel to each other. The brass was then taken out of the lathe and flipped and machined down until the two cylinders separated from each other. Then a Garolite disk was cut and through holes drilled. This allows the base to be easily attached to the brass cylinders and ring after they have been threaded for appropriately sized screws.

To measure the double layer capacitance of the ionic fluids, the fluid height in the capacitor was increased in 50µL steps using a micropipette. A handheld LCR meter was used to take individual data points which were then plotted in Origin. The relationship was expected to be linear as capacitance increases with fluid height.

Linear capacitance was measured from a handheld LCR meter and varied fluid height. From graphical analysis it became clear to begin analysis after the fluid has reached 500µL. This is because the parafilm seal in the macro device is hydrophobic and reaches a more reliable and uniform fluid level at 500µL. It was also noted that the linear relationship becomes stronger after 3mm of height.

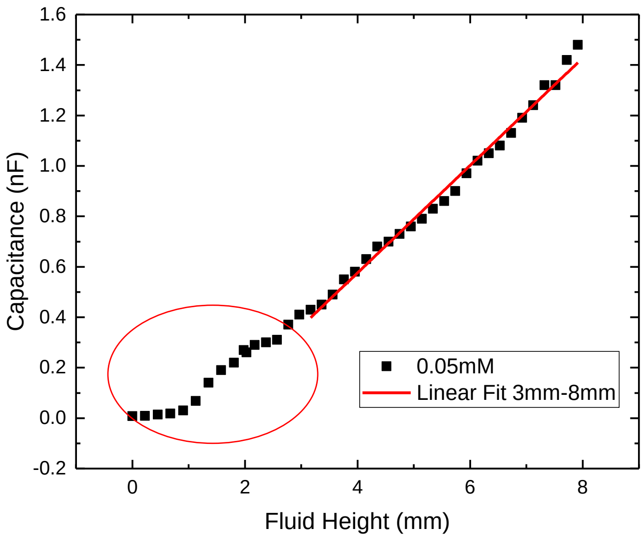

Figure 2.4: Sample data exhibiting a stable linear relationship after 3mm and the nonlinear climb from zero.

The experimental setup is shown in Figure 2.5. The fluid was stored in a non-conducting plastic tube. The tube did not have a flat base so a holder was machined to hold the tube.

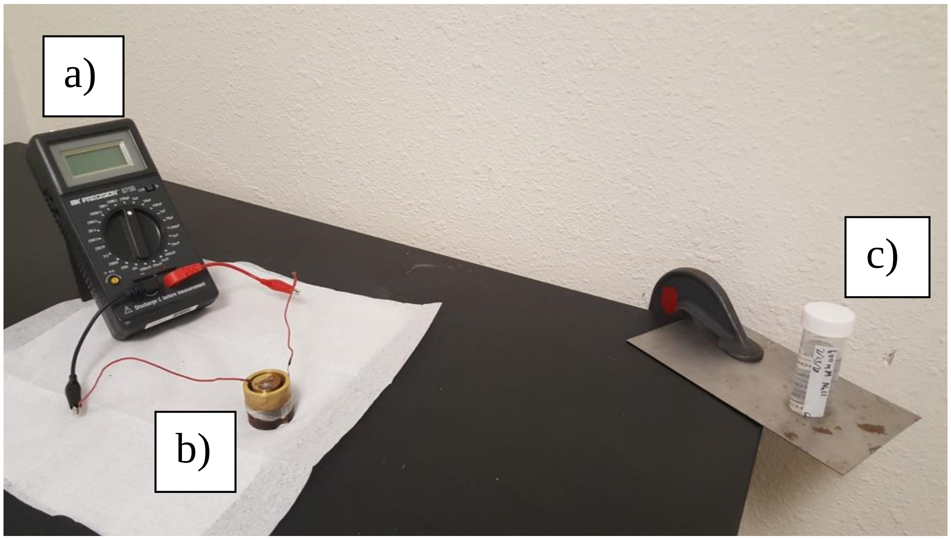

Figure 2.5: Image of experimental setup, a) handheld LCR meter, b) cylindrical capacitor, and c) fluid holder.

3. Theory

Double layer capacitance is an effective way to determine charge carrier density and electrolyte concentration. These relationships are well established in academic literature.

3.1 Cylindrical Capacitance

Cylindrical capacitance was chosen for this experiment because of its geometrical symmetry. The geometry of the system helps simplify the mathematics behind calculating capacitance. Cylindrical Capacitance is defined by equation 2 for a cylindrical capacitor with no dielectric.

$$\boldsymbol{C = \frac{2\pi\epsilon_0 \ell}{\ln\left(\frac{b}{a}\right)}} \tag{3}$$

Where ϵ_0 is the permittivity of free space, *a* is the inner radius, *b* is the outer radius and *l* is the height. To account for the material between the cylinders add dielectric constant, K for the fluid, to equation 2[3].

$$\boldsymbol{C = \frac{2\pi \mathrm{K} \epsilon_0 \ell}{\ln\left(\frac{b}{a}\right)}} \tag{4}$$

3.2 Double Layer Capacitors

Double layer capacitance is unique to fluid capacitors. This phenomenon occurs because of the different charge carriers in the materials with electrons in metal and ions in fluid. The charge of the metal causes the ions in the fluid to be attracted to the metal/fluid interface. The ions of the fluid then pile on until they reach a critical point where no more ions can fit at the interface. At this critical point, the distance from the edge of the metal to the edge of the ionic wall is called the Stern layer *x.* An additional distance which is the length it takes for the ions in the fluid to return to their normal ratio is called the Debye length, λ. The double layer capacitor is exclusively at the interface of the metal and fluid. The bulk electrolyte acts instead as a conductor for ionic charges[4]. See Figure 1.1 for reference.

3.2.1 Debye Length

The Debye-Huckel parameter or the Debye length can be calculated mathematically for individual fluids[3]. The equation for the Debye length is shown in equation 4[1],

$$\boldsymbol{\lambda = \left[\frac{N_A e^2}{\epsilon\epsilon_0 kT}\sum_i z_i^2 c_i\right]^{-1/2}} \tag{5}$$

where N_A is Avagadro's number, e is the charge of an electron, ϵ is relative permittivity ϵ_0 is vacuum permittivity, k is Boltzmann's constant, T is temperature, z is the atomic mass of the salt and c is the concentration. The *i* notation is to label which atom in the summation you are using for z, and what concentration it is at that atoms location, c. At T of 298 K, $\frac{N_A e^2}{\epsilon\epsilon_0 kT} = 5.404 \times 10^{15} m$.

3.2.2 Stern Layer

The Stern layer can be calculated from the size of the molecule that is resting at the surface of the metal. In the case of NaCl, Na ions attract to the negative side of the capacitor and Cl ions to the positive side. The Stern layer increases in size for longer molecule chains, whereas the Debye length only relies on the molecule's net charge.

3.3 Total Capacitance

In a cylindrical capacitor there will be double layer capacitors on both the inner and outer cylindrical surfaces. These can be treated as two capacitors in series:

$$\boldsymbol{C_{total} = \frac{1}{\frac{1}{C_1}+\frac{1}{C_2}} = \frac{C_1 C_2}{C_1 + C_2}} \tag{6}$$

Using equation 3 for cylindrical capacitors with a dielectric, and including the addition of the Debye length for each capacitor, C_1 and C_2 are defined as follows.

$$\boldsymbol{C_1 = \frac{2\pi\kappa\epsilon_0\ell}{\ln\left(\frac{a+\lambda}{a}\right)} \quad \& \quad C_2 = \frac{2\pi\kappa\epsilon_0\ell}{\ln\left(\frac{b-\lambda}{b}\right)}} \tag{7}$$

We can expand the natural log using a Taylor series to simplify the equations. This is possible because the terms are sufficiently small since λ is on the order of nanometers. These can then be evaluated and plugged back into equation 5 to yield:

$$\boldsymbol{C_{total} = \frac{2\pi\kappa\epsilon_0\ell ab}{\lambda(a+b)}} \tag{8}$$

From this and equations 3 and 6 it can be shown that:

$$\boldsymbol{\frac{C}{\ell} \propto \frac{1}{\lambda} \propto \sqrt{c}} \tag{9}$$

The total capacitance measurement then shows a $\sqrt{c}$ dependency because it also depends on λ[1]. These equations can be plotted in origin for comparison to the experimental results.

3.4 Stern Layer Inclusion

The model is missing the Stern layer and the inclusion in the equation is derived below.

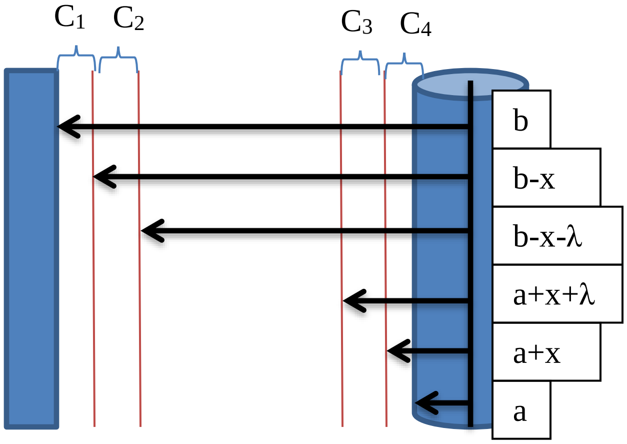

Figure 3.1: Diagram of capacitor distances in the macroscopic device. Note a is the inner radius, b is the outer radius, x is the width of the Stern layer, and λ is the Debye length.

The total capacitance in the system can be written as the sum of the Debye and Stern capacitors in series[1].

$$\frac{1}{C_{Total}}=\frac{1}{C_{Debye}}+\frac{1}{C_{Stern}}=\frac{C_{Debye}C_{Stern}}{C_{Debye}+C_{Stern}} \qquad \textbf{(10)}$$

From Figure 3.1

$$\frac{1}{C_{Debye}}=\frac{C_2C_3}{C_2+C_3}\ \&\ \frac{1}{C_{Stern}}=\frac{C_1C_4}{C_1+C_4} \qquad \textbf{(11)}$$

Then evaluating these for a cylindrical capacitor with respective distances, and using the Taylor series simplification from 3.3[7]

$$C_1=\frac{2\pi\kappa\epsilon_0\ell b}{x_1} \qquad \textbf{(12)}$$

$$C_2=\frac{2\pi\kappa\epsilon_0\ell b}{\lambda} \qquad \textbf{(13)}$$

$$C_3=\frac{2\pi\kappa\epsilon_0\ell a}{\lambda} \qquad \textbf{(14)}$$

$$C_4=\frac{2\pi\kappa\epsilon_0\ell a}{x_2} \qquad \textbf{(15)}$$

For C_2 and C_3 the Stern distance is approximately absorbed into b and a respectively because of the order of magnitude difference. These can be plugged into equation 11

$$\frac{1}{C_{Debye}}=\frac{C_2C_3}{C_2+C_3}=\frac{2\pi\kappa\epsilon_0\ell ba}{\lambda(b+a)} \qquad \textbf{(16)}$$

$$\frac{1}{C_{Stern}} = \frac{C_1 C_4}{C_1 + C_4} = \frac{2\pi\kappa\epsilon_0 \ell ba}{bx_2 + ax_1} \qquad \textbf{(17)}$$

This now solves equation 10

$$\frac{1}{C_{Total}} = \frac{C_{Debye} C_{Stern}}{C_{Debye} + C_{Stern}} = \frac{2\pi\kappa\epsilon_0 \ell ba}{(bx_2 + ax_1)\big(\lambda(b+a)\big)} \qquad \textbf{(18)}$$

This model now includes both Stern and Debye. In a simplified case with only the dielectric and distances it can be shown that:

$$\frac{C_{Debye} C_{Stern}}{C_{Debye} + C_{Stern}} = \gamma \frac{\left(\frac{70}{\lambda}\right)\left(\frac{6\ or\ 70}{0.2}\right)}{\left(\frac{70}{\lambda}\right) + \left(\frac{6\ or\ 70}{0.2}\right)} \qquad \textbf{(19)}$$

Where ϒ is the constants shared, and λ is the Debye length. For most cases the Stern layer is the width of a single ion, i.e. 0.2 nm. The number in the numerator is the dielectric constant, where 70 is the dielectric constant for water and 6 is the dielectric constant for the Stern layer if the ions are so compact that they push the fluid out[7]. It can be seen that the Stern layer will be larger, because the concentration of fluids will not reach a level where the dielectric would drop to 6. This shows that the Debye contribution in the denominator would absorb into the Stern contribution and thus the Stern portion would effectively cancel with the Stern in the numerator. Because of this, even in accounting for the Stern layer a $\sqrt{c}$ dependence is still expected.

4. Results & Analysis

The linear capacitance relationship and $\sqrt{c}$ dependency was analyzed for three different ionic fluids. Theoretical lines and fits come from the expected relationship as discussed in the theory section. Origin was used to graph all data sets and analyzed for standard deviation and error. The slopes of each linear concentration is plotted to find the $\sqrt{c}$ dependency that is expected.

4.1 NaCl

NaCl is composed of a positive Na and a negative Cl. Using the method from Dr. Pallab Ghosh[3] the expected theory line can be computed for the Debye length. Since the ion sizes are comparable the Debye length is believed to be the dominant factor in the capacitance measurement.

4.1.1 Linear Capacitance

The relationships of each fluid's capacitance with respect to fluid height are strongly linear. This can be seen in Figure 4.1. It is important to note that the figure is on a log vs log scale.

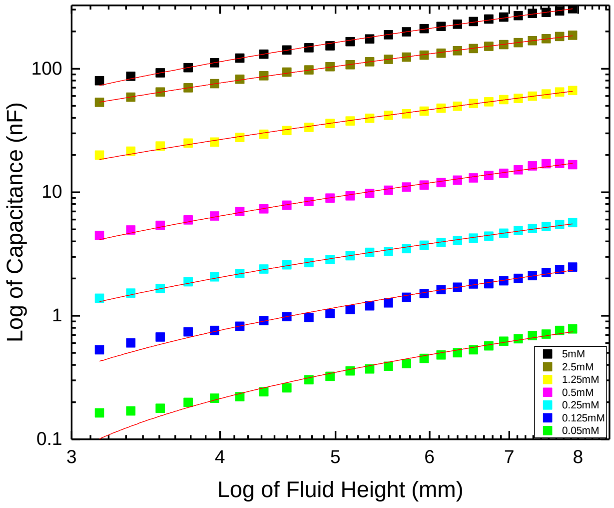

Figure 4.1: NaCl capacitance measurements of fluid concentrations from 0.05mM to 5mM.

4.1.2 $\sqrt{c}$ Dependency

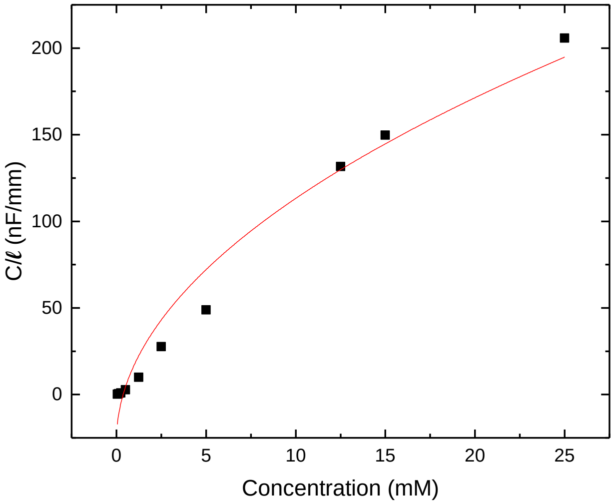

Figure 4.2: $\sqrt{c}$ fit of slopes from each data set from Figure 4.1.

As can be seen in Figure 4.2 the slope of each capacitance measurement does not have a strong correlation with the expected $\sqrt{c}$ dependency.

4.2 Phosphate

The phosphate buffer, with chemical formula KH_2PO_4 has K as the cation and H_2PO_4 as the anion.

4.2.1 Linear Capacitance

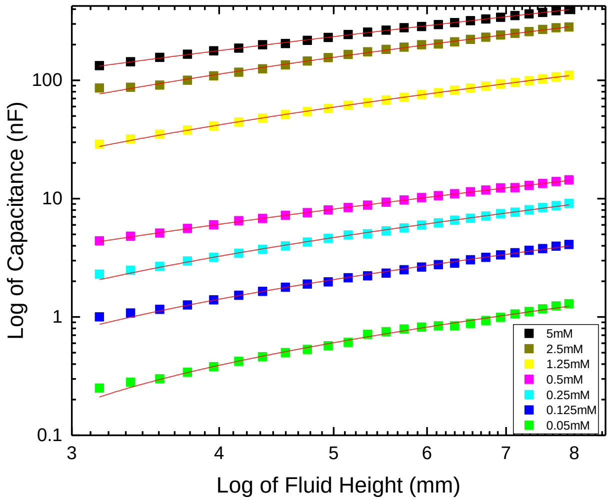

Figure 4.3: Linear capacitance measurements for Phosphate of concentrations 0.05Mm through 5mM.

4.2.2 $\sqrt{c}$ Dependency

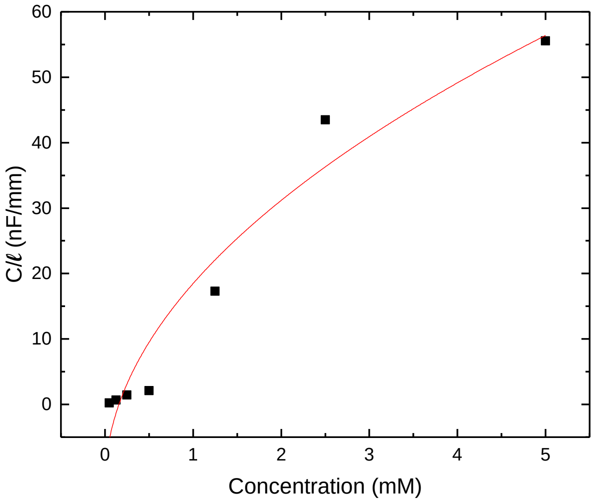

Figure 4.4: $\sqrt{c}$ fit of slopes from Figure 4.3 for Phosphate.

4.3 HEPES

HEPES is a biological salt, $C_8H_{18}N_2O_4S$. The same calculations and analysis are performed as noted above.

4.3.1 Linear Capacitance

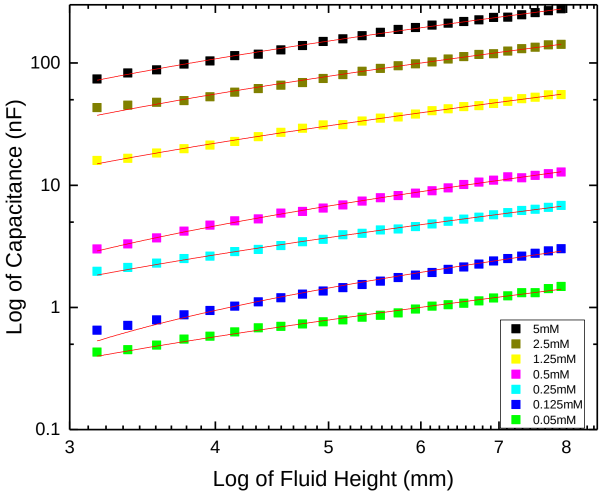

Figure 4.5: Linear capacitance measurements from 0.05mM to 5mM.

4.3.2 $\sqrt{c}$ Dependency

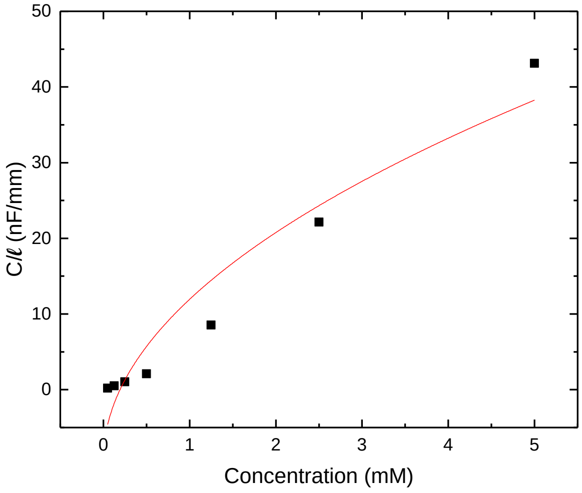

Figure 4.6: $\sqrt{c}$ fit of slopes from Figure 4.5 for HEPES.

The fit in Figure 4.6 is not as strong as in NaCl, Figure 4.2. This could be from a stronger dependence on the Stern layer or device contamination.

4.4 Discussion

Our results show the expected linear correlation between capacitance and fluid height. The $\sqrt{c}$ fit is strongest in NaCl and weak in the Phosphate and HEPES. This may be due to the complicated nature of double layer capacitance. As described above, double layer capacitance depends on two factors, the Stern layer and the Debye length. In simpler electrolytes, like NaCl, it is enough to only rely on the $\sqrt{c}$ dependency of the Debye length. However, even with the inclusion of the Stern layer we would still expect $\sqrt{c}$ dependency. This may mean that our model is omitting some other key detail to the fluid capacitor system as a whole. This model also did not include quantum capacitance as it should be negligible at this scale[8].

5. Conclusion

The goal of this thesis was to accurately model the behaviors of ionic fluids in double layer capacitors. A cylindrical capacitor was used to take measurements of various fluids at varied concentrations. It was shown that capacitance was linearly dependent on fluid height and showed a $\sqrt{c}$ dependence in NaCl. However, this model was not effective for the Phosphate or HEPES.

A further addition to this thesis could be more fluid concentrations as well as a more accurate technique for measuring higher concentrated fluids. Much of this thesis focused on low concentrations but work on higher order concentrations could yield interesting trends. Including more fluid types could also help characterize their behaviors.

Further work can be done on effectively modeling the fluid behavior with both the Debye length and Stern layer modelled. More investigation can be done on other effects that could be happening in the device. Effective modeling for double layer capacitance would help check data accuracy as well as make predictive models for other fluids.

6. Acknowledgements

In concluding this document I would be remiss if I did not thank all of the wonderful individuals that have helped me along my journey. First I would like to thank Linfield and the Faculty Student Collaborative Research Grant without which this thesis could not have been written. I would like to thank Dr. Michael Crosser for his guidance and patience, there were many bumps along the road and he greatly helped get me to where I am today. I would like to acknowledge the incredible Linfield Physics Department, both students and faculty. They provided me with a family here at Linfield that I could always turn to. I would especially like to thank Aggie for all of the laughs and memories we shared in Graf. Thank you to my wonderful thesis committee, without whom you would not be reading this thesis. Finally I would like to thank all of my family and friends for their unwavering love and support as I take my next steps on my journey in the pursuit of knowledge, and a better tomorrow.

7. Bibliography

1. Ghosh, P. *Electrostatic Double Layer Force: Part II* . Joint Initiative of IITs and IISc
2. Heller, I. et al. Influence of electrolyte composition on liquid-gated carbon nanotube and graphene transistors. J. Am. Chem. Soc. **132**, 17149–56 (2010).
3. Nave, R. Cylindrical Capacitor. *Hyper Physics* Available at: http://hyperphysics.phy-astr.gsu.edu/hbase/electric/capcyl.html. (Accessed: 15th July 2017)
4. Ponomarenko, L. A. et al. Effect of a high-κ environment on charge carrier mobility in graphene. Phys. Rev. Lett. **102**, 100–103 (2009).
5. Sanchez, C. et al. Liquid-Mediated Dense Integration of Graphene Materials for Compact Capacitive Energy Storage. Science. **341**, 534–537 (2013).
6. Shandle, J. Supercapacitors Find Applications in Hybrid Vehicles, Smartphones, and Energy Harvesting. Mouser Electronics - Electronic Components Distributor Available at: https://www.mouser.com/applications/new-supercapacitor-applications/. (Accessed: 8th April 2018)
7. Velikonja, A., Gongadze, E., Kralj-Iglič, V. & Iglič, A. Charge Dependent Capacitance of Stern Layer and Capacitance of Electrode/Electrolyte Interface. International Journal of Electrochemical Science. **9**, 5885–5894 (2014).
8. Xia, J., Chen, F., Li, J. & Tao, N. Measurement of the quantum capacitance of graphene. Nat. Nanotechnol. **4**, 505–509 (2009).